

## Research Article

# Effects of Frequency and Temperature on Optimum Dimensions of a Quantum Well Solar Cell (AlGaAs/GaAs)

Mamadou Lamine Diallo<sup>\*</sup> , Papa Gueye Ndiaye , Mor Ndiaye, Gaye Kharma , Papa Touty Traore , Issa Diagne

Department of Physics, Semiconductor Laboratory, Cheikh Anta Diop University of Dakar, Dakar, Senegal

## Abstract

In this work, we studied the effect of frequency and temperature on the optimal dimensions of a quantum well photodiode made of an alloy of materials (AlGaAs/GaAs). In fact, the derivative of the photocurrent density with respect to the recombination velocity at the junction ( $S_f$ ) gives a quadratic equation whose solutions are expressions of the recombination velocities ( $Se_1$  and  $Se_2$ ) at the front surface. Thus, by analyzing the mathematical expressions describing the recombination rates of charge carriers in the solar cell, the graphical representation of these relationships based on different parameters, such as operating frequency and temperature, allows the optimal thickness to be precisely determined, maximizing energy conversion efficiency while minimizing recombination losses. Finally, analysis of these curves made it possible to establish calibration relationships for the optimal thickness, thus providing a reliable prediction of the solar cell's behavior and the material's efficiency. The calibration curves obtained provide a solid basis for studying system performance, optimizing manufacturing processes and adjusting production parameters. This approach improves the efficiency of quantum well solar cells through precise characterization, with the aim of maximizing their energy yield.

## Keywords

Quantum Well Solar Cell, Recombination Speed, Optimal Thickness, Temperature and Frequency

## 1. Introduction

Faced with pollution problems and the limits of fossil fuels, the interest in renewable energies is generating major commitment [1]. Due to the low efficiency of silicon photovoltaic cells, many studies have been devoted to identifying factors limiting their efficiency [2, 3]. This is how it is in the search for the highest yields obtained by photovoltaic conversion, quantum well solar cells based on gallium arsenide are proving to be among the most promising. The GaAs band gap width ( $E_g = 1.425$  eV) is close to that required to achieve the highest solar conversion efficiency [4, 5]. The performance of

solar cells is strongly influenced by high temperature [6] which affects performance. Quantum well solar cells are less influenced by high operating temperatures and are better suited for epitaxial crystallization for the growth of ternary or quaternary semiconductor alloys. This has led to the phenomenon of development of multi-junction solar cells [7]. Thus, solar cells with low thickness obtained with heterojunctions present real advantages for improving efficiency. However, solar cells are optimized taking into account dy-

<sup>\*</sup>Corresponding author: Mamadoulaminodiallo41@gmail.com (Mamadou Lamine Diallo)

**Received:** 22 May 2025; **Accepted:** 9 June 2025; **Published:** 30 June 2025



Copyright: © The Author(s), 2025. Published by Science Publishing Group. This is an Open Access article, distributed under the terms of the Creative Commons Attribution 4.0 License (<http://creativecommons.org/licenses/by/4.0/>), which permits unrestricted use, distribution and reproduction in any medium, provided the original work is properly cited.

namic  $D(w, T)$ , temperature  $(T)$  [8-10] dependent diffusion coefficient, frequency  $(w)$  [11, 12] as well as recombination rates.

This work aims to determine the optimal thickness of the emitter of a quantum well solar  $(n^+ pp^+)$  cell under monochromatic illumination in dynamic frequency regime for different temperatures.

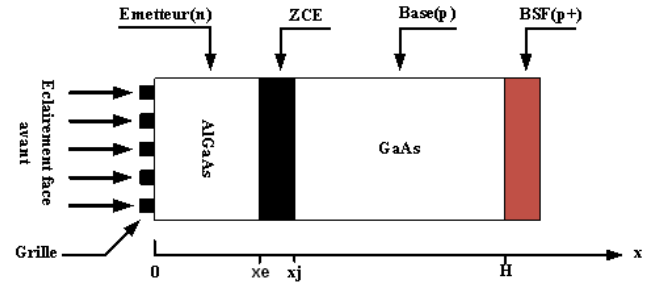


Figure 1. Structure of a quantum well solar cell.

## 2. Theoretical Study

The study focuses on a quantum well solar cell of the  $npp^+$  type under monochromatic illumination represented by the figure below.

Considering the phenomena of recombination, diffusion and generation in the solar cell illuminated by monochromatic light, electron-hole pairs are created. The continuity equation of excess minority charge  $\delta(x, \omega, T)$  carriers in the dynamic frequency regime is given by the following relation (1):

$$D(\omega, T) * \frac{\partial^2 \delta_n(x, t, \omega, T)}{\partial x^2} - \frac{\delta_n(x, t, \omega, T)}{\tau} = -G_n(x, t, \omega, T) + \frac{\partial \delta_n(x, t, \omega, T)}{\partial t} \quad (1)$$

$\delta(x, t, \omega, T)$  is the density of excess minority charge carriers which can be written in the form.

$$\delta_n(x, t, \omega, T) = \delta_n(x, \omega, T) \exp(i\omega t)$$

With  $\delta_n(x, \omega, T)$  the spatial component and the temporal component.

$G_n(x, t, \omega, T)$  is the carrier generation [13, 14] rate which is given by the expression:

$$G_n(x, t, \omega, T) = g_n(x, \omega, T) \exp(i\omega t)$$

With  $g_n(x, \omega, T)$  the spatial component  $e^{i\omega t}$  and the temporal component. We have:

$$g_n(x, \omega, T) = \alpha F(\lambda) (1 - R(\lambda)) \exp(-\alpha x)$$

$D^*(\omega, T)$  is the complex diffusion coefficient of excess minority carriers. Its expression is given by [15-18, 12]:

$$D^*(\omega, T) = D(T) \cdot \left[ \frac{1 - j\omega^2 \tau^2}{1 + (\omega \tau)^2} \right]$$

With  $D(T)$  is the diffusion coefficient of the electron carriers given by the relation below:

$$D(T) = \frac{\mu(T) \cdot K_b \cdot T}{q}$$

1)  $\mu(T) = 1,43.10^{19} T^{-2,42}$  is the electron mobility coefficient [9, 19, 20]

2)  $K_b$  is the Boltzmann coefficient

3)  $T$  is the temperature

4)  $q$  is the elementary charge of the electron

$L^*(\omega, T)$  is the complex diffusion coefficient of the excess minority carriers is given by:

$$L^*(\omega, T) = \frac{L(T)}{\sqrt{1 + i\omega \tau}}$$

With  $L(T) = \sqrt{D(T) \cdot \tau}$  is the diffusion length of excess minority carriers.

The solution of the equation (1) allows us to obtain the expression of the density of the minority carriers  $\delta(x, \omega, T)$  is of the form:

$$\delta(x, \omega, T) = A \cosh\left(\frac{x}{L^*(\omega, T)}\right) + B \sinh\left(\frac{x}{L^*(\omega, T)}\right) - K \exp(-\alpha x) \quad (2)$$

$$\text{with } K = \frac{\alpha L^{*2}(\omega, T) F(\lambda) (1 - R(\lambda))}{D^{*2}(\omega, T) (\alpha^2 L^{*2}(\lambda) - 1)}$$

With the boundary conditions, we can determine the constants A and B.

Boundary conditions:

On the front side:  $x = 0$

$$\left. \frac{\partial \delta(x, \omega, T)}{\partial x} \right|_{x=0} = \frac{S_e}{D^*(\omega, T)} \delta(x, \omega, T) \Big|_{x=0} \quad (3)$$

With  $S_f$  the speed of recombination of minority carriers on the front face.

At the junction boundary:  $x = x_e$

$$\left. \frac{\partial \delta(x, \omega, T)}{\partial x} \right|_{x=x_e} = -\frac{S_f}{D^*(\omega, T)} \delta(x, \omega, T) \Big|_{x=x_e} \quad (4)$$

With  $S_e$  the recombination speed of minority carriers on the front side.

Solving equations (3) and (4), we obtain two equations with two unknowns of A and B. the solution of this system leads to the determination of the expressions of A and B.

The expression of the recombination rate is determined from the photocurrent density which depends on the density of the excess minority carriers  $\delta(x, T, \lambda)$  (2) which translates into the following relation:

$$J(S_f, \omega, T) = -qD^*(\omega, T) \left. \frac{\partial \delta(x, T, \lambda)}{\partial x} \right|_{x_e} \quad (5)$$

From the relation, the equation for the determination of recombination rates is obtained. Knowing that for large values of the recombination rate of the charge carriers at the junction, the photocurrent density is constant. It corresponds to the short-circuit current [21, 22]. Consequently, its derivative with respect to the recombination velocity ( $S_f$ ) is zero:

$$\left. \frac{\partial J_{ph}(S_f, \omega, T)}{\partial S_f} \right|_{S_f \rightarrow grand} = 0 \quad (6)$$

This derivative allows us to obtain two expressions of the recombination rate of the front face ( $S_{e1}$ ) and ( $S_{e2}$ ).

### 3. Results and Discussions

The optimum thickness of the emitter is obtained by the intersection of the two curves relating to the recombination rates ( $S_{e1}$ ) and ( $S_{e2}$ ).

#### 3.1. Determination of the Optimum Thickness of a Quantum Well Solar Cell for Different Temperature Values at Low Frequency

Figure 2 below shows the recombination rates for different

temperature values with  $f=1,75.10^2 \text{ Hz}$ :

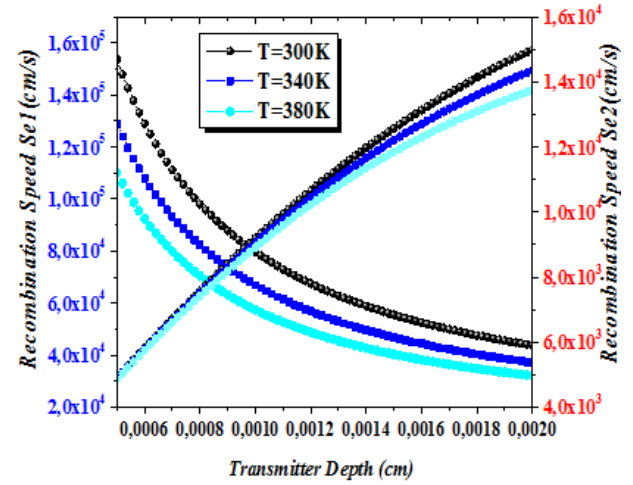


**Figure 2.** Front face recombination speed as a function of emitter thickness for different temperature values  $f=1,75.10^2 \text{ Hz}$ .

The intersection of the curves ( $Se1$ ) and ( $Se2$ ), gives the thickness of the solar cell emitter for each value of the low-frequency temperature. Thus, from these data, the table below is established:

**Table 1.** The values shown above represent the optimum thickness of the emitter for different temperatures.

Temperature (K)	Optimum thickness (Cm). $10^{-4}$
300	9.689
340	8.919
380	8.483

Table 1 shows the optimum thickness as a function of temperature at low frequency.

Figure 3 shows that the optimal thickness decreases with increasing temperature for a low frequency. Indeed, when the temperature rises, the density of photogenerated carriers (electrons and holes created by the absorption of light) increases. As a result, the difference between the concentrations of majority and minority carriers decreases, which reduces the relative density of minority carriers in the material. This reduction directly influences the photocurrent density, which is the current generated by the photovoltaic effect. This allows the wearers to travel a greater distance before disappearing. Therefore, a thinner thickness is sufficient to efficiently collect these carriers, which is why the optimal thickness decreases with temperature.

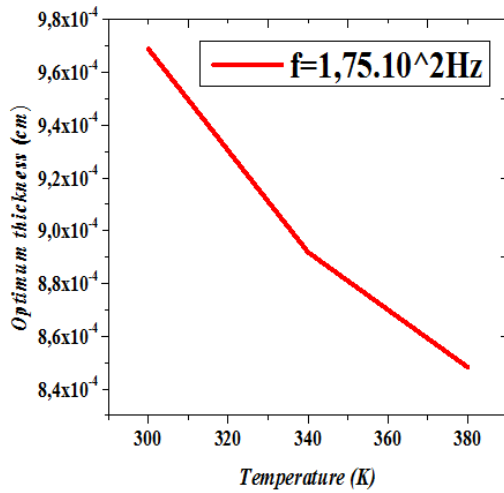


Figure 3. Optimum thickness according to temperature.

The calibration relationship between temperature ( $T$ ) in kelvin and optimum thickness ( $H_{op}$ ) in  $10^{-4} \text{ cm}$  is given by the following formula:

$$H_{op} = 2,1 \cdot 10^{-5} T^2 - 0,02045 T + 13,409$$

### 3.2. Determination of the Optimum Thickness of a Quantum Well Solar Cell for Different High-frequency Temperature Values

Figure 4 below illustrates the recombination speeds for different temperature values with  $f=3,75 \cdot 10^6 \text{ Hz}$ :

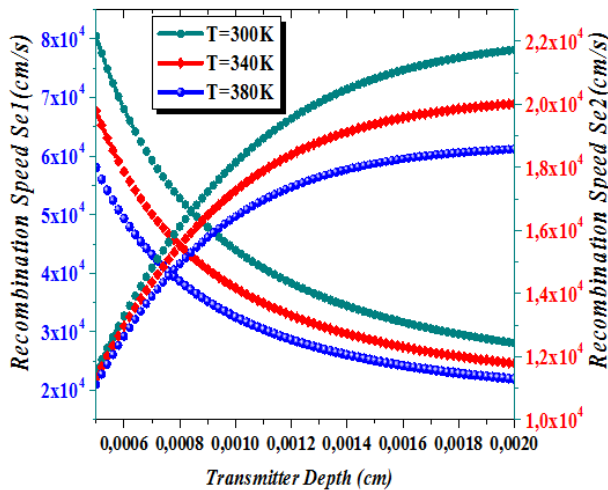


Figure 4. Front face recombination speed as a function of emitter.

On the basis of the results in Figure 4, we draw up the table below:

Table 2. The values shown above represent the optimum thickness of the emitter for different temperature values,  $f=3,75 \cdot 10^6 \text{ Hz}$ .

Temperature (K)	Optimum thickness (Cm). $10^{-4}$
300	8.407
340	7.975
380	7.710

Table 2 shows the optimum thickness as a function of temperature at high frequency.

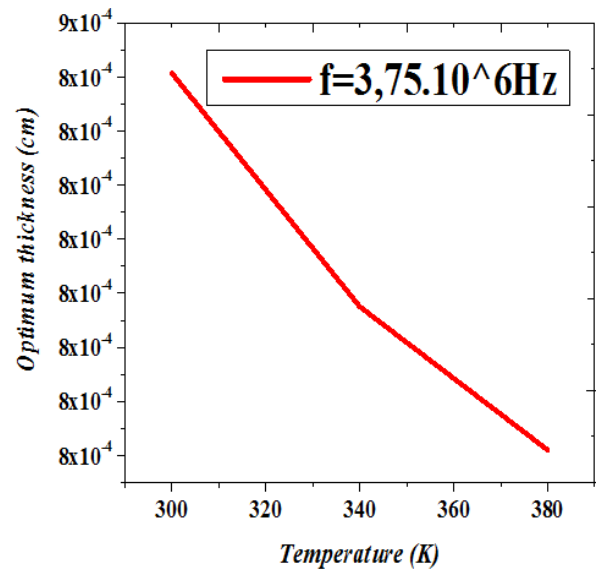


Figure 5. Optimum thickness according to temperature.

Figure 5 illustrates that the optimum thickness decreases slightly with increasing temperature, particularly for high values of the frequency. This phenomenon is explained by the increase in the density of photogenerated carriers with temperature, leading to a reduction in minority carriers. Indeed, at high frequencies, photons have enough energy, thus they absorbed close to the surface of the material. In addition, increasing the temperature increases optimum efficiency with a reduced thickness of material to capture most of the light.

The calibration relationship that relates the temperature ( $T$ ) in Kelvin to the optimal thickness ( $H_{op}$ ) in  $10^{-4} \text{ cm}$  the material is expressed by a functional relationship of the following form:

$$H_{op} = 5,22 \cdot 10^{-5} T - 0,0442 T + 16,9701$$

### 3.3. Determination of the Optimum Thickness of a Quantum Well Solar Cell for Different Frequency Values at Low Temperatures

Figure 6 below illustrates the recombination rates as a function of different frequency values with  $T = 300K$ :

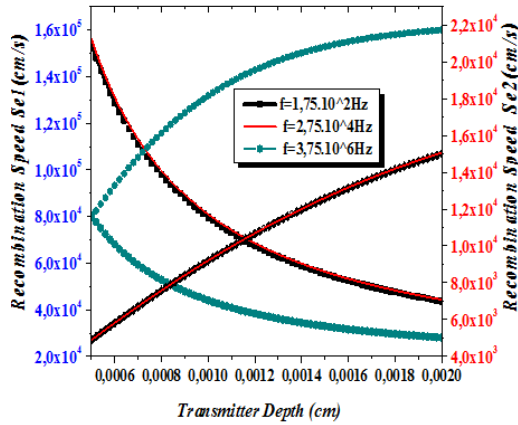


Figure 6. Front face recombination speed as a function of emitter thickness for different frequency values,  $T = 300K$

The table below shows the results of Figure 6:

Table 3. The values shown above represent the optimum thickness of the transmitter for different frequency values,  $T = 300K$ .

Frequency (Hz)	Optimum thickness (Cm). $10^{-3}$
$1,75.10^2$	1,026
$2,75.10^4$	1,024
$3,75.10^6$	0,5047

Table 3 allows to represent the optimal thickness as a function of frequency at low temperature,  $T = 300K$ .

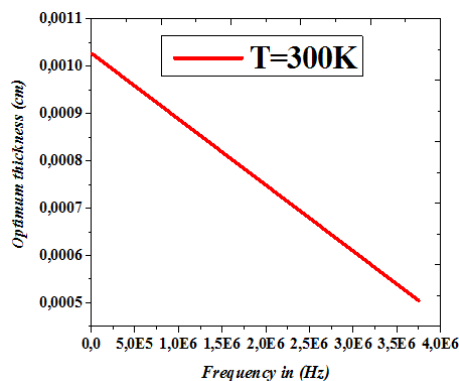


Figure 7. Optimal Thickness as a Function of Frequency.

The profile in Figure 7 shows that the optimal thickness decreases with increasing frequency for low temperature values. This is because at higher frequencies, photons interact easily with the material (AlGaAs), resulting in more efficient absorption of photons even at relatively low temperatures. In other words, the higher the frequency, the greater the energy of the photons, the more energy the photogenerated carriers capture, which can increase their diffusion in the material. Thus, a reduction in the optimum thickness of the material (AlGaAs) observed.

The calibration relationship between frequency ( $f$ ) in Hz and optimum thickness ( $H_{op}$ ) in cm is deduced from the results in Table 3.

$$H_{op} = -1,39.10^{-7} f + 1,026$$

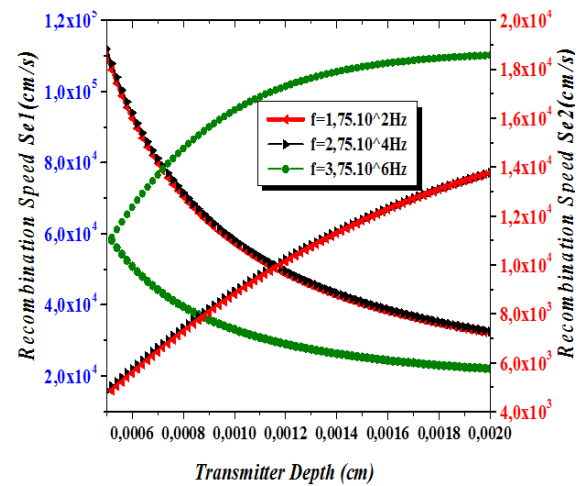


Figure 8. Vitesse de recombinaison de la face avant en fonction de l'épaisseur de l'émetteur pour différentes valeurs de fréquence,  $T = 380K$

The results in Figure 8 give the table below:

Table 4. The values shown above represent the optimum thickness of the emitter for different frequency values,  $T = 380K$ .

Frequency (Hz)	Optimum thickness (Cm). $10^{-3}$
$1,75.10^2$	1,074
$2,75.10^4$	1,061
$3,75.10^6$	0,5213

Table 4 allows to represent the optimal thickness as a function of frequency at high temperature.

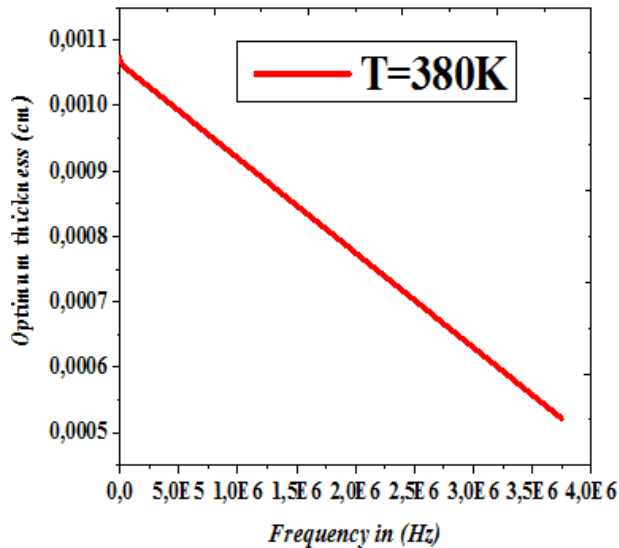


**Figure 9.** Optimum thickness as a function of frequency.

According to [Figure 9](#), the optimal thickness decreases with increasing frequency at high temperatures. When the temperature is high, the bandgap width of the semiconductor decreases. Thus, the photons are absorbed by the AlGaAs material more efficiently. It has been observed that the optimum thickness decreases with increasing frequency, particularly at high temperatures. This can be explained by the fact that at high temperatures, the band gap of the semiconductor (AlGaAs) decreases. Indeed, when the forbidden band is narrower, lower-energy photons (corresponding to higher frequencies) can excite electrons from the valence band to the conduction band. This reduction of the forbidden band allows photons to be absorbed more efficiently in the material (AlGaAs). As a result, the optimal thickness of the material decreases with an increase in frequency, particularly at high temperatures where the energy gap is smaller.

The calibration relationship linking the frequency ( $f$ ) in Hz to the optimum thickness ( $H_{op}$ ) in cm, based on the data in [Table 4](#), is as follows:

$$H_{op} = -1,47.10^{-7} f + 1,589$$

## 4. Conclusions

In this study of the quantum well solar cell emitter, a method was developed to determine the optimum thickness by analyzing the intercession of the recombination velocities.

As the temperature increases, the available energy allows for greater excitation of charge carriers, which enhances the impact of photon absorption. Even at low frequencies, the increase in temperature can favor the creation of photogenerated carriers. A thin layer of material is therefore sufficient to collect these carriers, as their density is high and recombina-

tion losses are minimized. However, at high frequencies, photons have a higher energy and interact more effectively with the material. This leads to stronger absorption and more localized generation of carriers near the surface. By analyzing calibration curves, it is possible to simulate system performance and adjust production processes, with in-depth characterization aimed at maximizing the efficiency of photovoltaic cells.

Finally, the calibration curves obtained predict the behavior of the systems and optimize the solar cell manufacturing processes with detailed characterization for improved efficiency.

## Abbreviations

K	Kelvin
$H_{op}$	Optimal Thickness
$K_b$	Boltzmann Coefficient

## Author Contributions

**Mamadou Lamine Diallo:** Conceptualization, Funding acquisition, Investigation, Methodology, Software, Visualization, Writing - original draft

**Papa Gueye Ndiaye:** Resources, Visualization

**Gaye Kharma:** Resources

**Papa Touty Traore:** Resources, Writing - review & editing

## Conflicts of Interest

The authors declare no conflicts of interest.

## References

- [1] Howard Geller, "Energy Revolution", Renewable Energy World, 6/4, 34-49 (2003).
- [2] C. T. Sah, 'High Efficiency Crystalline Silicon Solar Cells' Solar Cells, 17, pp. 1-27, 1986.
- [3] J. R. Hauser and P. M. Dunbar, 'Performance Limitations of Silicon Solar Cells', IEEE Trans. on Elec. Devices ED-24, N 4, pp. 305-321, 1977.
- [4] WOODALL, J. M. and HOVEL, H. J., Appl. Phys. Lett. 30 (1977) 492.
- [5] SAHAI, R., EDWALL, D. D. and HARRIS, J. S. Jr., Appl. Phys. Lett. 34 (1979) 147.
- [6] S. Shao, H. et Lu, Temperature dependence of photovoltaic cell efficiency: A review. Energy Reports, 2021, 7, 293-306.
- [7] B. Li, X. B. Xiang, Z. P. Y ou, Y. Xu, X. Y. Fei, X. B. Liao, High efficiency AlxGal\_xAs/GaAs solarcells: Fabrication, irradiation and annealing effect, Sol. EnergyMater. Sol. Cells44(1996)63-67.



- [8] E. Gaubas and J. Vanhellemont, "A simple technique for the separation of bulk and surface recombination parameters in silicon," *J. Appl. Phys.*, vol. 80, no. 11, pp. 6293-6297, Dec. 1996, <https://doi.org/10.1063/1.363705>
- [9] J. M. Dorkel and P. Leturcq, "Carrier mobilities in silicon semi-empirically related to temperature, doping and injection level," *Solid. State. Electron.*, vol. 24, no. 9, pp. 821-825, Sep. 1981, [https://doi.org/10.1016/0038-1101\(81\)90097-6](https://doi.org/10.1016/0038-1101(81)90097-6)
- [10] R. Mane *et al.*, "Minority Carrier Diffusion Coefficient  $D^*(B, T)$ : Study in Temperature on a Silicon Solar Cell under Magnetic Field," *Energy Power Eng.*, vol. 9, no. 1, pp. 1-10, Jan. 2017, <https://doi.org/10.4236/EPE.2017.91001>
- [11] S. Diouf *et al.*, "Influence of Temperature and Frequency on Minority Carrier Diffusion Coefficient in a Silicon Solar Cell under Magnetic Field," *Energy Power Eng.*, vol. 11, no. 10, pp. 355-361, Oct. 2019, <https://doi.org/10.4236/EPE.2019.1110023>
- [12] A. Mandelis, "Coupled ac photocurrent and photothermal reflectance response theory of semiconducting p - n junctions. I," *J. Appl. Phys.*, vol. 66, no. 11, pp. 5572-5583, Dec. 1989, <https://doi.org/10.1063/1.343662>
- [13] F. Ahmed and S. Garg, International Centre for Theoretical Physics (ICTP), Trieste, ITALY, Internal Report, Août 1986
- [14] Andreas Mandelis *J. Appl. Phys.* Vol. 66 No. 11, 1 December, 1989, pp. 5572-5583.
- [15] M. F. M. Fall *et al.*, « Vitesse de recombinaison de la surface arrière AC dans une cellule solaire en silicium n+-p-p+ sous une lumière et une température monochromatiques », *J. Electromagn. Anal. Appl.* vol. 13, n° 5, pp. 67-81, juil.2021, <https://doi.org/10.4236/JEMAA.2021.135005>
- [16] D. Kabou *et al.*, "AC BACK SURFACE RECOMBINATION IN N+-P-P+ SILICON SOLAR CELL: EFFECT OF TEMPERATURE," *Int. J. Adv. Res.*, vol. 8, no. 7, pp. 140-151, Jul. 2020, <https://doi.org/10.21474/IJAR01/11273>
- [17] C. H. Wang *et al.*, « Mesure de la durée de vie et de la vitesse de recombinaison de surface des porteurs minoritaires par photoluminescence dans le domaine fréquentiel », *IEEE Trans. Electron Devices*, vol. 38, n° 9, p. 2169-2180, 1991, <https://doi.org/10.1109/16.83745>
- [18] S. Gupta, F. Ahmed *et al.*, « Une méthode pour la détermination des paramètres matériels  $\tau$ , D, L0, S et  $\alpha$  à partir du photocourant de court-circuit CA mesuré », *Sol. Cells*, vol. 25, n° 1, pp. 61-72, octobre 1988, [https://doi.org/10.1016/0379-6787\(88\)90058-0](https://doi.org/10.1016/0379-6787(88)90058-0)
- [19] Arora, N. D. and Hauser, J. R. (1982) Temperature Dependence of Silicon Solar Cell Characteristics. *Solar Energy Materials*, 6,151-158. [https://doi.org/10.1016/0165-1633\(82\)90016-8](https://doi.org/10.1016/0165-1633(82)90016-8)
- [20] Kunst, M. and Sanders, A. (1992) Transport of Excess Carriers in Silicon Wafers. *Semiconductor Science and Technology*, 7, 51-59. <https://doi.org/10.1088/0268-1242/7/1/009>
- [21] Sissoko, G., Museruka, C., Corréa, A., Gaye, I. And Ndiaye, A. L. (1996), « Light Spectral Effect on Recombination Parameters of Silicon Solar Cell », *World Renewable Energy Congress*, Pergamon, Part III, pp. 1487-1490.
- [22] Diallo, H. L., Maiga, S. A., Wereme, A. and Sissoko, G. (2008), New Approach of Both Junction and Back Surface Recombination Velocities in a 3D Modelling Study of a Polycrystalline Silicon Solar Cell. *The European Physical Journal Applied Physics*, 42, 203-211. <https://doi.org/10.1051/epjap:2008085>